

New $^{207}\text{Pb}/^{206}\text{Pb}$ -Zr minimum evaporation, metamorphic $^{87}\text{Rb}/^{86}\text{Sr}$ -WR-Bt ages and tectonic imprints in the Archean So'o Group (Ntem Complex/Congo Craton, SW Cameroon)

S. OWONA, J. M. ONDOA, M. TICHOMIROWA, L. RATSCHBACHER, F. M. TCHOUA AND G. E. EKODECK

Received 3 March 2011; Revision Accepted 9 May 2011)

ABSTRACT

New ages were obtained from charnockites and tonalites collected in the So'o Group in the Ntem Complex. The rocks were analyzed for their petrography, tectonics and $^{207}\text{Pb}/^{206}\text{Pb}$ zircon minimum ages of their zircons as well as metamorphic $^{87}\text{Rb}/^{86}\text{Sr}$ isochron ages. The charnockites yielded zircon ages with a mean value of 2739 ± 18 Ma interpreted as their intrusion age. This age is in agreement with previously published zircon Archean ages of charnockites and TTG from the NC. The So'o Group has been subjected to the D_1 N-S compression emplacing the S_1 sub-vertical foliation and L_1 lineation, followed by a D_2 E-W compression. The D_2 induced subgrain reduction, area reduction feldspar and quartz dynamic recrystallization, N-S large-scale F_2 folds and an "Archean nappe" on a large-scale. The charnockites and tonalites metamorphic $^{87}\text{Rb}/^{86}\text{Sr}$ ages were significantly younger than the Archean $^{207}\text{Pb}/^{206}\text{Pb}$ zircon ages, showing that they were overprinted by later processes. Metamorphic $^{87}\text{Rb}/^{86}\text{Sr}$ isochron ages of charnockites and tonalites differ. The older age of 1969 ± 170 Ma, which corresponds to the Eburnean orogeny (2400~1800 Ma) was obtained in charnockites located near the Nyong Complex emplaced during the Congo-São Francisco craton collision. The younger $^{87}\text{Rb}/^{86}\text{Sr}$ isochron age of 1129 ± 13 Ma, determined in tonalites located close to the border of the Yaounde Group represents the Kibarian/Greevalian orogeny. Both $^{87}\text{Rb}/^{86}\text{Sr}$ isochron ages are assigned to the Eburnean and Kibarian/Greevalian cooling ages respectively.

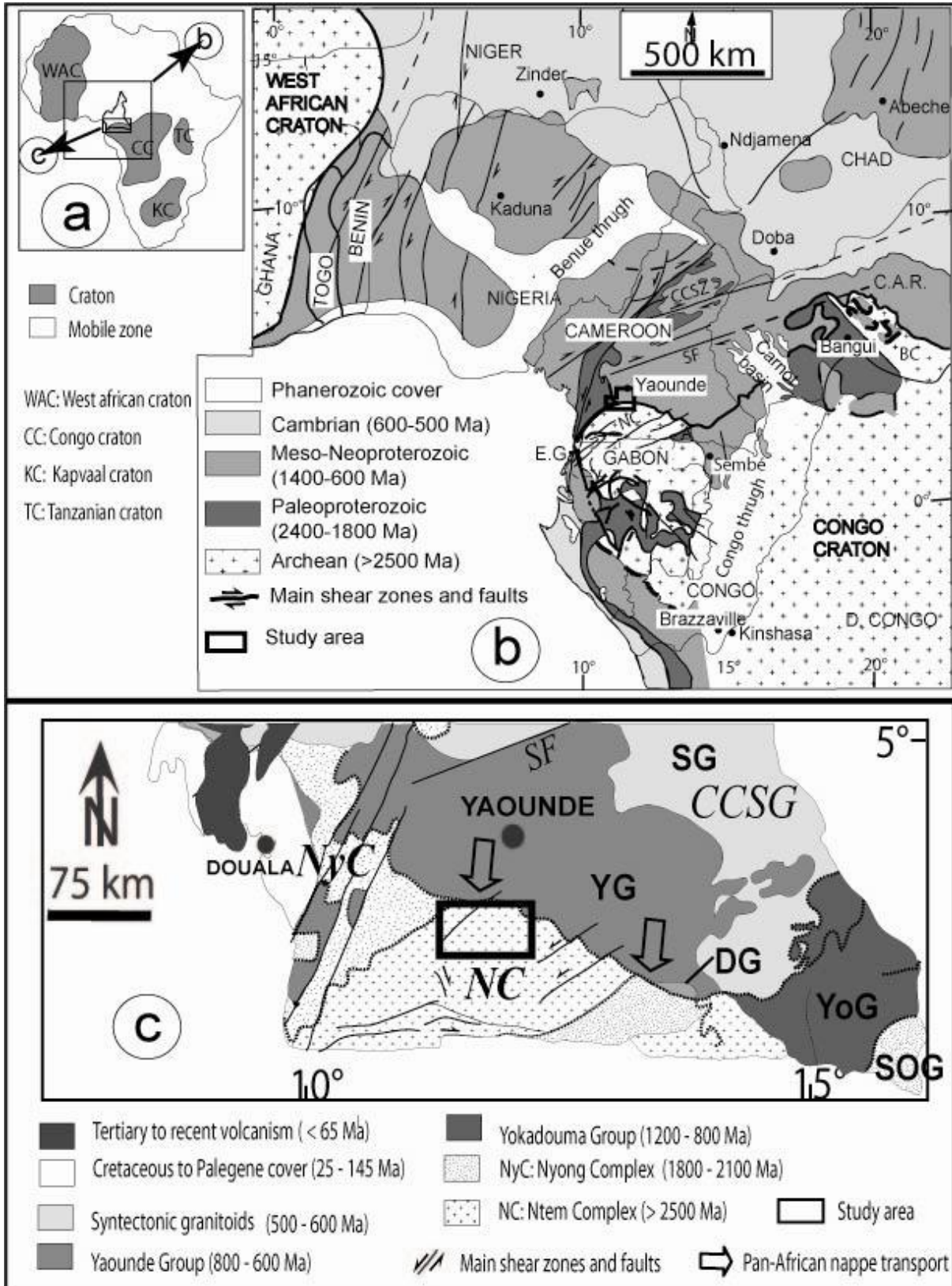
KEY WORDS: Archean, Eburnean, Kibarian/Greevalian, Ntem complex, Cameroon

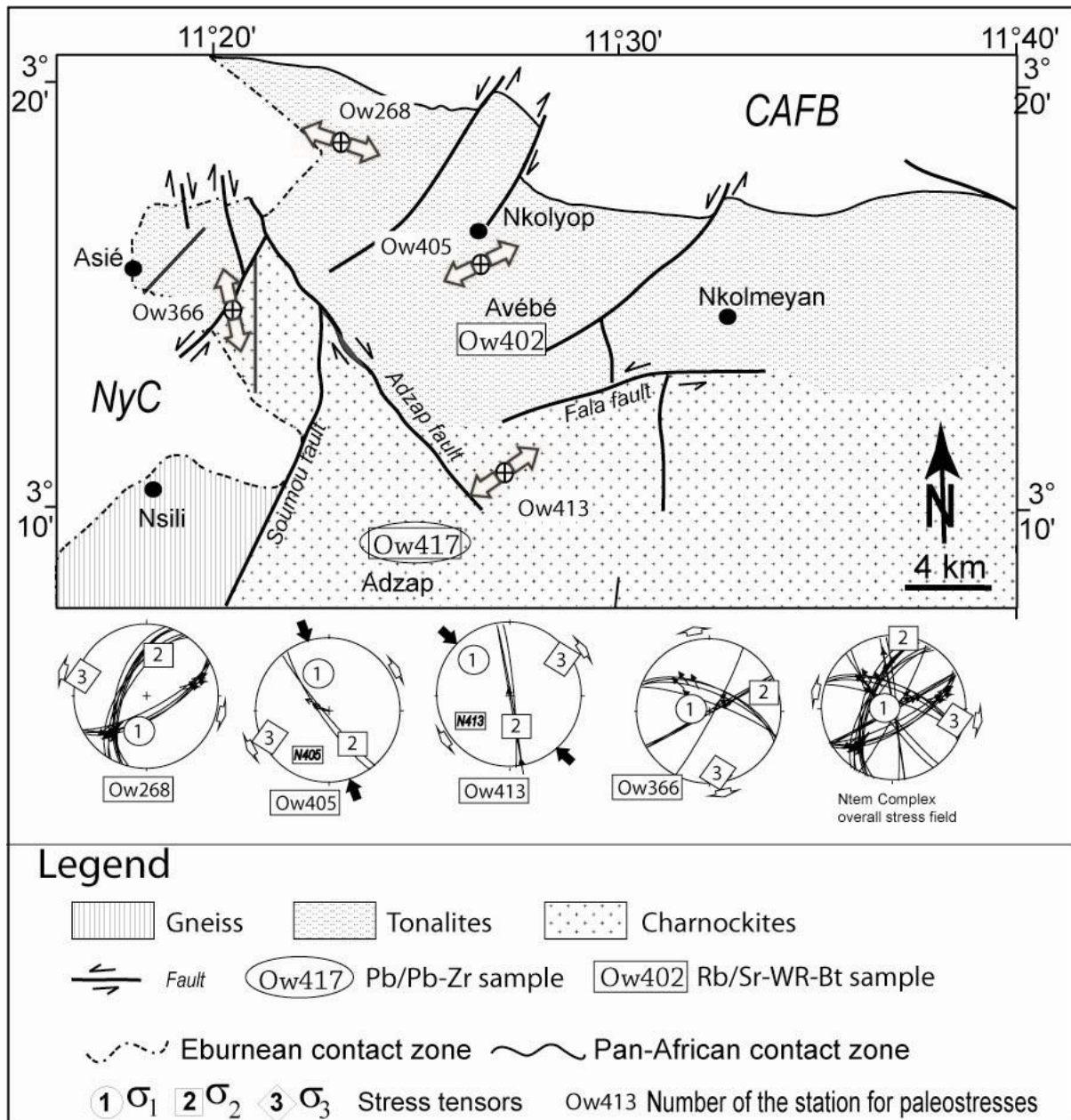
1. INTRODUCTION

The Ntem Complex (NC) is the Cameroonian part of the NW Congo Craton (CC, Fig. 1; Champetier de Ribes and Aubagne, 1956; Maurizot *et al.*, 1986; Trompette, 1994; Feybesse *et al.*, 1998). It consists of charnockite, monzogranite, syenogranite, tonalite, trondhjemite, granodiorite (TTG), syenite and band iron formation (BIF), greenstone-belt type, migmatite and granulitic gneiss. The TTG are differentiated into charnockitic, granodioritic, and tonalitic suites (Fig. 2; Nédélec *et al.*, 1990; Nsifa and Riou, 1990; Tchameni, 1997; Shang, 2001) that intruded according to concordant U/Pb zircon dating between 3.3 and 2.7 Ga (Caen-Vachette, 1988; Toteu *et al.*, 1994b; Tchameni *et al.*, 2000; Tchameni *et al.*, 2001; Shang *et al.*, 2004a, b, 2010). In the studied So'o Group, rocks are constituted of charnockite, monzogranite, syenogranite, TTG, syenite and BIF. Their geochemistry has been widely described. It suggests subduction as the main tectonic model (Nédélec *et al.*, 1990; Tchameni *et al.*, 2000; Tchameni *et al.*, 2001; Shang *et al.*, 2001b; 2004a, b, Shang *et al.*, 2006). As the NC and the whole NW Congo craton, the So'o Group was also subjected to two main phases of metamorphism including the gneissification episode [e.g. Haute Noya and Mitzic-Oyem gneiss in the Mont de Cristal Complex in Gabon (Caen-Vachette *et al.*, 1988) as well as Ebolowa gneiss in the NC (Lasserre and Soba, 1976a recalculated in Caen-Vachette *et al.*, 1988)]

and the charnockitization (Caen-Vachette *et al.*, 1988; Toteu *et al.*, 1994b; Tchameni, 1997). Despite their stability, these rocks were affected by ductile and brittle deformations (D_n). The D_1 deformation was described as a non-rotational, showed hypersolidus textures and S_1 foliation (Nsifa *et al.*, 1993; Feybesse *et al.*, 1998). The D_2 deformation known as a coaxial tectonics is underlined by the S_2 foliation, F_2 folds and C_2 sinistral shear planes (Owona, 2008; Owona *et al.*, 2011b). The sub-vertical S_2 foliation was observed in the relict greenstones belts and TTG series while sinistral C_2 shear planes trend N-S to N45E - N50E was associated with a partial melting of the TTG and greenstones belt country rocks (Tchameni, 1997; Feybesse *et al.*, 1998; Shang, 2001; Shang *et al.*, 2004a, b; Owona, 2008; Owona *et al.*, 2011b). D_3 - D_4 showed transcurent tectonics in the NC (Tchameni *et al.*, 2001), represented by several C_3 mylonitic and shear corridors (Shang *et al.*, 2004a). While the petrography, geochemistry of charnockites and TTG main rock types have been characterized (Tchameni, 1997; Shang, 2001; Shang *et al.*, 2004a, b; Owona, 2008), the mineralogy and associated pressure-temperature-deformation-age (P-T-d-t) conditions are still poorly described. The present study aims at highlighting the 1/50.000 geological map of the So'o Group (the available ones have scales ranging from 1:1.000.000 to 1:500.000), new discussions on its petrography, tectonic imprints and geochronology in a regional geodynamic context.

Sébastien. Owona, Department of Earth Sciences, Faculty of Science, University of Douala, P.O. Box. 24157, Douala, Cameroon*
Joseph. M. Ondoa, Department of Earth Sciences, Faculty of Science, University of Yaounde, P.O. Box. 812, Cameroon
Marion. Tichomirowa, Institute of Mineralogy, TU Bergakademie Freiberg, Brennhaugasse 14, D-09596 Freiberg, Germany
Lothar. Ratschbacher, Institute of Geology, TU Bergakademie Freiberg, Zeunerstr. 12, D-09596 Freiberg, Germany
Felix. M. Tchoua, Institute of Geology, TU Bergakademie Freiberg, Zeunerstr. 12, D-09596 Freiberg, Germany
G. E. Ekodeck, Department of Earth Sciences, Faculty of Science, University of Douala, P.O. Box. 24157, Douala, Cameroon





2. Methods

Lithological types were surveyed, studied in outcrops, hand sample and in thin sections. The major structural elements as the foliations, lineations, axial planes, fold axes, shear planes and faults were identified. The S_n foliations include as possible the S_0 bedding, lithological and metamorphic S_n layering. The L_n lineations include the stretching and mineral types. The F_n folds studied are cartographic. The faults were measured through their strikes, dips and associated slickensides. The pole of the S_n foliation, the L_n lineations, the S_{n+1} axial planes and A_{n+1} fold axes as reference directions were plotted in an equal area of the lower hemisphere in the SPHESISTAT stereographic projection. (See the [Stesky R.M., Spheristat User's Manual, Pangaea Scientific, Brockville, Ontario, Canada](#)). Planar structures are in the Dip/Dip-direction e.g. 45/273 and linear structures in the Dip-direction/Dip e.g. 273/45 forms. For fault slip analysis, we calculated the orientation of principal stress axes and the reduced stress tensors (e.g., [Angelier,](#)

1984) with the computer Turbo Pascal program packages of [Sperner et al. \(1993\)](#) and [Sperner and Ratschbacher \(1994\)](#). (See Appendix B for details in [Ratschbacher et al. \(2003\)](#)).

Single zircons from samples of charnockites were analyzed in the Isotopenlabor of the Technische Universität Bergakademie Freiberg in Germany. The analytical technique is an evaporation technique developed by [Kober \(1987\)](#), detailed in [Tichomirowa et al. \(2001\)](#). In this method, a single zircon grain of 125 – 250 μm size mounted on rhenium filaments was “cleaned” for 10 minutes by heating at 1450 °C. This should remove common Lead from cracks and discordant parts of the zircon. Then the zircon grain was evaporated and the Pb transferred to the second filament during a single cycle at 1600 °C. Pb was then ionized at temperatures between 1190 – 1220 °C and, the ^{207}Pb , ^{206}Pb and ^{204}Pb isotopes were analysed in a FINNIGAN MAT 262 using dynamic SEM ion counter. Ion beam intensities were measured in 10 blocks of 9

scans. The $^{207}\text{Pb}/^{206}\text{Pb}$ ratios were corrected for (1) common lead derived from the $^{204}\text{Pb}/^{206}\text{Pb}$ ratios, following the two-stage Pb isotope evolution model of [Stacey and Kramers \(1975\)](#) and (2) fractionation and mass-bias of 0.0036 per amu involving of the spectrometer, determined through repeated analyses of zircon standards. The values obtained 1064.9 ± 2.1 Ma ($n=13$) were checked by repeated analysis of the zircon standards 91500 and 380.3 ± 1.9 Ma for the standard S-2-87 (accepted age 381.5 ± 4.0 Ma) Wenham Monzonite (Geological Survey of United States, [Wiedenbeck, 1995](#)). After evaluation of outliers and the corrections mentioned above, a mean ratio of $^{207}\text{Pb}/^{206}\text{Pb}_{\text{corr}}$ was gained from a single zircon measurement (Table 1). Apparent zircon ages were produced by iteration of the two system equations of the decay chains $^{238}\text{U}/^{206}\text{Pb}$ and $^{235}\text{U}/^{207}\text{Pb}$; the error on the single zircon age was calculated as 2 standard errors of the mean (2σ mean), using the mean ratio of $^{207}\text{Pb}/^{206}\text{Pb}_{\text{corr}}$ and the error of the measured ratios (calculation program Isotopengeochemisches Labor der Technische Universität Bergakademie Freiberg/Sachsen). For the age estimation, it is important to obtain reproducible ages by analysis of several zircons from the same sample, because the calculated $^{207}\text{Pb}/^{206}\text{Pb}$ ages are model ages with no information about concordance or the degree of discordance. Given that these ages resulted from high-temperature evaporation with no significant changes in the $^{207}\text{Pb}/^{206}\text{Pb}$ ratios, the data points are concordant or nearly so. In addition, we suggest on a statistical basis that when 5 – 7 zircon ages from one sample fall within a similar range, this should be considered as dating a zircon magmatic crystallization event. The single zircon

isotopic data was evaluated by the weighted mean ages; corresponding error from a zircon population has been plotted in a single variable diagram. A weighted mean age calculated ([Ludwig, 2001](#)) from this population was determined by this method, and by definition, corresponds to minimum ages. This method has been successfully applied in magmatic, metamorphic and sedimentary terrains and checked with U/Pb ages ([Tichomirowa et al., 2001](#)). Analytical results are given in Table 1 and Figure 3a.

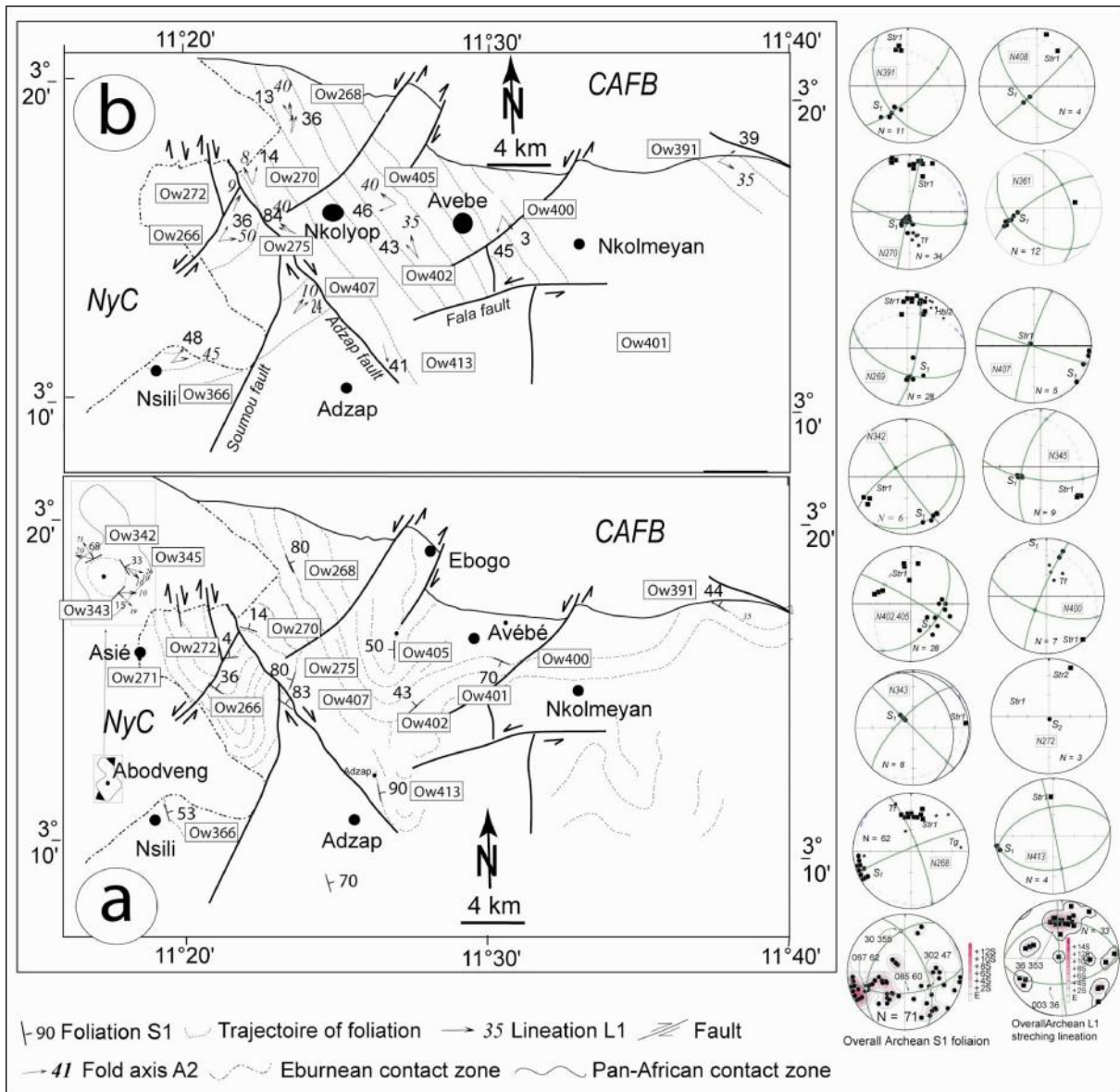
For Sr isotope analyses, about 50 mg of whole-rock sample powder was spiked with mixed $^{84}\text{Sr}/^{87}\text{Rb}$ tracers prior to dissolution in $\text{HF}+\text{HNO}_3$ acid at 120°C , under high pressure in polytetrafluor-ethylene (PTFE) reaction bombs. Element separation (Rb, Sr) was performed in quartz columns containing a 4ml resin bed of AG 50W-X8, 100–200 mesh, conditioned and equilibrated with 2.5N HCl. For mass spectrometric analyses, Sr and Rb was loaded with phosphoric acid and measured on a single Ta filament. All analyses were performed using a FINNIGAN MAT 262 thermal ionisation mass spectrometer (TIMS) equipped with 8 Faraday cups in a static collection mode. $^{87}\text{Sr}/^{86}\text{Sr}$ ratios were normalized to $^{86}\text{Sr}/^{88}\text{Sr} = 0.1194$ derived for the year 2007. Within the same period, the NBS 987 Sr standard yielded $^{87}\text{Sr}/^{86}\text{Sr}$ ratio of 0.71029. Total procedural blanks (chemistry and loading), were $<200\text{pg}$ for Sr and Rb. Least-square regression of Rb/Sr isotopic data with assessment of fit using mean square of weighted deviates (MSWD), were calculated using ISOPLOT program of [Ludwig \(2001\)](#). All regression errors are quoted at 2σ . Biotite and muscovite samples were separated by their magnetic properties. Analytical results are given in Table 2 and Figure 3b, c.

Table 1: Pb isotopic data from single grain zircon evaporation for Pb/Pb-Zr ages

| Sample | Zircon morphology | Grain | Mass scan | $^{204}\text{Pb}/^{206}\text{Pb}$ b | 2σ error | $^{207}\text{Pb}/^{206}\text{Pb}$ b | 2- σ error | $^{207}\text{Pb}/^{206}\text{Pb}$ ^{206}Pb age | 2- σ error |
|--------|---|------------|-----------|--|-----------------|--|-------------------|--|-------------------|
| Ow417 | Long-prismatic, idiomorphic, yellow to pink | Ow417z11 | 89 | 0.001210 | 0.000016 | 0.187970 | 0.000225 | 2724.4 | 1.8 |
| | | Ow417Z9 | 90 | 0.001420 | 0.000013 | 0.188280 | 0.000165 | 2727.2 | 1.4 |
| | | Ow417Z7 | 17 | 0.001260 | 0.000207 | 0.186900 | 0.002370 | 2722.8 | 15.1 |
| | | Ow417Z1 | 89 | 0.000975 | 0.000029 | 0.189500 | 0.000546 | 2736.8 | 4.3 |
| | | Ow417Z12 | 89 | 0.000883 | 0.000029 | 0.190820 | 0.000491 | 2748.4 | 4.0 |
| | | Ow417Z6 | 90 | 0.000873 | 0.000012 | 0.192370 | 0.000221 | 2762.5 | 6.9 |
| Mean | | Six grains | 464 | 0.001104 | 0.000051 | 0.189307 | 0.000670 | 2737.0 | 5.6 |
| | | | 77.33 | | | Isoplot mean with total correction | | 2739.0 \pm 18.0 Ma | |

Table 2: Rb and Sr isotopic data for Rb/Sr isochron ages

| Samples | Rb [ppm] | Sr [ppm] | $^{87}\text{Sr}/^{86}\text{Sr}$ | $^{87}\text{Rb}/^{86}\text{Sr}$ | WR-Bt-age | $^{87}\text{Sr}/^{86}\text{Sr}(i)$ |
|---------------------|----------|----------|---------------------------------|---------------------------------|-----------------------|------------------------------------|
| Ow417 (Charnockite) | | | | | | |
| WR | 56.1 | 571.0 | 0.71361 | 0.285 | 1969 \pm 1 70 Ma | 0.7105 \pm 0.13 |
| Bt-3 | 543.0 | 19.3 | 3.66942 | 104.810 | | |
| Bt-4 | 535.0 | 31.1 | 2.35768 | 57.800 | | |
| Ow402 (Tonalite) | | | | | | |
| WR | 7.0 | 762.0 | 0.70270 | 0.027 | 1129 \pm 1 3 Ma | 0.70227 \pm 0.00028 |
| Bt1-1 | 68.6 | 22.5 | 0.84723 | 8.940 | | |
| Bt-2 | 70.1 | 24.3 | 0.83972 | 8.460 | | |
| Bt-1-3 | 73.3 | 19.9 | 0.87523 | 10.810 | | |



3. RESULTS

a. Petrography

The So'o Group (Fig. 2a) consists of tonalites, charnockites, gneisses and norites (Fig. 2; Nédélec *et al.*, 1990; Tchameni, 1997; Tchameni *et al.* 2001; Owona, 2008). Only the charnockites (Ow417, GPS 11°27'11" N and 3°14'22" E) and tonalites (Ow402 GPS, 11°22'16" N and 3°09'43"E) were analyzed in this study. Charnockites are pink and isotropic in outcrop while feldspar and quartz could be identified in hand specimen. In thin section, they contain quartz (35-30%), plagioclase (25-30%), hypersthene (20-25%), microcline (5-10%), green amphibole (5%) and biotite (2%). Hypersthene (0.5-1 mm) forms subhedral grains with quartz, biotite and opaque inclusions. The quartz (<0.2 mm) presents undulose and patchy extinction. It shows recrystallized rims including micrometric sub grains forming subgrain rotation (SGR) fabrics (Photo 1a) and inclusions in blasts and subhedral (0.5-1 mm) grains. Plagioclase (An₁₀₋₁₅) is represented by subhedral poikiloblasts (1-2 mm). It is altered to epidote. Microcline consists of anhedral blasts (1mm). It is saussuritized to

epidote from its cracks and rims to the core. Feldspars define SGR grains where old magmatic cores are continuously replaced by new grains. Amphibole (0.2-0.5 mm) includes euhedral grains in the matrix. Biotite (0.2 mm) is kinked and surrounds hornblende. Apatite and zircon are inclusions in biotite, pyroxene and plagioclase. Epidote and sericite derived from the transformation of feldspar and calcite, and from amphibole. In general, charnockites are made of two mineral associations including magmatic and blast minerals. Magmatic minerals are represented by Pl+Hyp+Qtz+Bt±Op±Zr±Ap. Blasts are recrystallized Pl+Amf+Bt+Qtz. Ultimate retrogression is represented by Ep±Ca±Ser.

Tonalites are pale-green and isotropic in outcrops and hand sample in which feldspar and quartz are recognizable. Under the microscope, they are constituted of plagioclase (60-65%), quartz (15-20%), phlogopite (5-10%), diopside (5%), opaque (2%), sericite and epidote. Plagioclase (An₃₀₋₃₅) is represented by subhedral grains (0.5-1.5 mm) containing zircon and opaque as inclusions. It shows a less pronounced SGR microtexture. Quartz is represented by subhedral and

polycrystalline grains (0.2-1 mm), forming the sub grain area reduction (SGAR) recrystallized fabric with undulose and patchy extinction (Photo 1b). Phlogopite (0.2-0.5 mm) comprises opaque inclusions. Diopside (0.2-1 mm) is represented by subhedral grains transformed into amphibole. Apatite and zircon (0.2-0.5 mm) are euhedral and are present in the matrix. In general, the tonalites define magmatic (Pl+Di+Qtz+Bt±Op±Zr±Ap) and recrystallized (Pl+Amp+Bt+Qtz±Op) fabrics. The ultimate retrogression is represented by Ep±Ca±Ser.

b. Structure

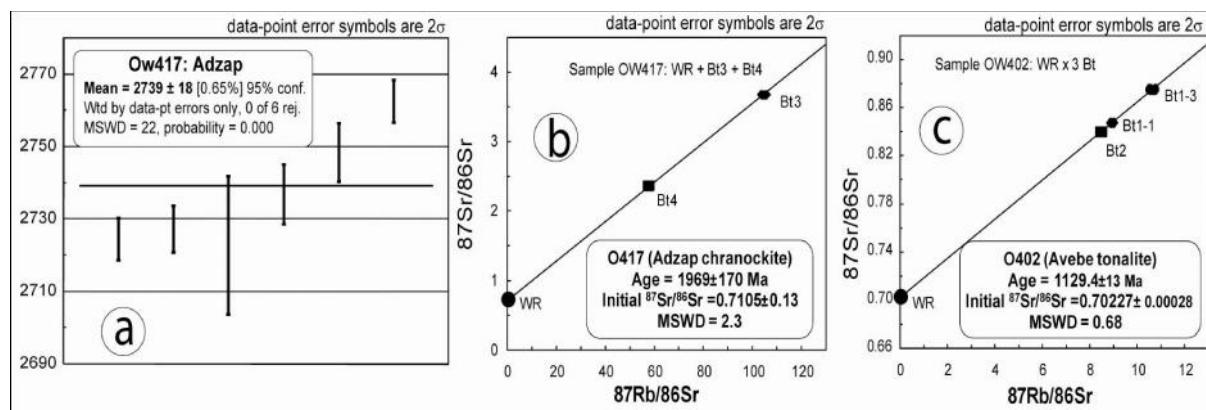
The D₁, D₂ and D₃₋₄ deformation phases affected the NC as well as ductile and brittle episodes (Champetier de Ribes and Aubague 1956; Maurizot *et al.* 1986; Tchameni, 1997; Tchameni *et al.* 2001; Shang 2001; Shang *et al.* 2004b). D₁ is represented by the S₁ foliation, L₁ lineation and F₁ folds. The S₁ foliation in outcrops is sub-vertical, displayed by the greywackes, BIF, sillimanite-bearing paragneisses and amphibolite layers (Shang *et al.* 2006). The S₁ foliation is oriented from NNW-SSE to E-W on both sides of the Adzap fault (Fig. 3a). It defines two average values, 62/067 and 42/302, suggesting a regional and large-scale folding. Greywackes, BIF, sillimanite-bearing paragneisses and amphibolite S₀ layers are folded in F₁ folds. The L₁ stretching lineation is oriented SE-NW to W-E (Fig. 3b). L₁ trajectories are locally reoriented W-E in the western side of Adzap fault. It is parallel to secant A₂ fold axis with 353/36 average value. D₂ is represented by meso- and large-scale F₂ folds inferred from S₁ foliation trajectories. These F₂ folds are tight to open sub-N-S synclines suggesting a regional E-W compression. The regional folding is oriented ca 60/085 (Fig. 3a). During

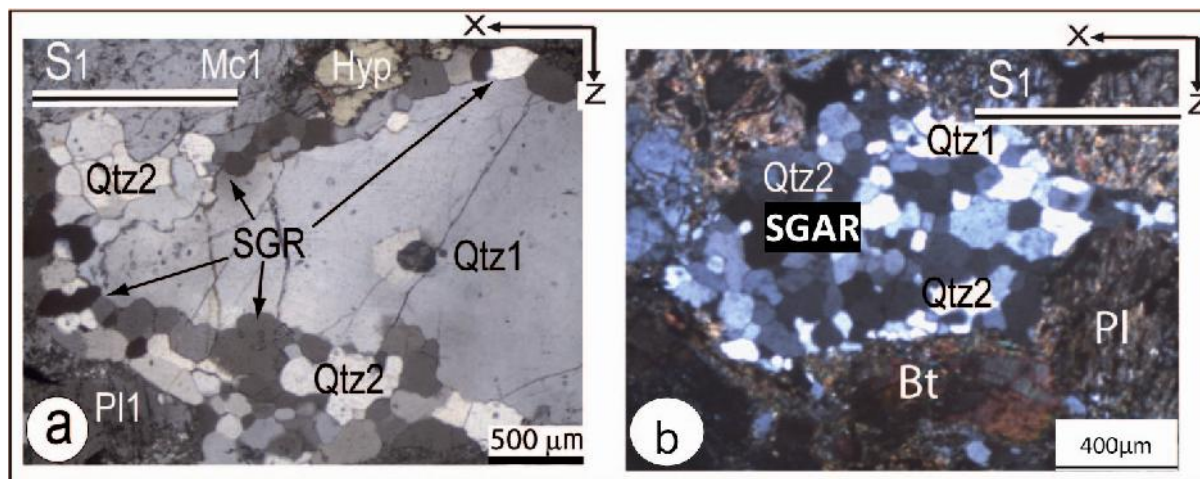
D₂, NC rock types recorded dynamic recrystallization (Kurse *et al.*, 2001; Stipp *et al.*, 2002; Passchier and Trouw, 2005) as the bulging (BLG), subgrain rotation (SGR) and subgrain area reduction (SGAR) are similar to Adzap charnockites and Avebe tonalites (Photo 1a, b). The D₃₋₄ is represented by faults defining important valleys and guiding hydrographical patterns (Owona, 2008). Brittle deformation is represented by normal dip-slip faults oriented NNE-SSW, NNW-SSE, WNW-ESE and ENE-WSW generated by a sub-vertical shortening according to the overall principal stress tensor σ_1 and σ_3 accompanied by a sub-E-W extension (Fig. 3b).

c. Geochronology

Table 1, 2, Fig. 4

The single sample dated for the ²⁰⁷Pb/²⁰⁶Pb zircon is Ow417 from Adzap charnockites (Table 1). The selected zircons were long-prismatic with slightly rounded terminations, without core, and with colour ranging from yellow to pink. Six grains without core yielded reproducible Archean ²⁰⁷Pb/²⁰⁶Pb ages between 2762±6.9 Ma and 2722±15.1 Ma, with a weighted mean 2737±5.6 and an isoplot mean with total correction of 2739±18 Ma (Fig. 4a). ⁸⁷Rb/⁸⁶Sr isotopes were obtained from the whole-rock and biotite separates (Table 2). The analyzed samples were Ow417 from Adzap charnockite and Ow402 from Avebe tonalite. In Ow417, the best fit correlation was determined, combining WR, Bt-3 and Bt-4. They yielded at 1969±170 Ma, MSWD = 2.3, with an initial ⁸⁷Sr/⁸⁶Sr ratio of 0.7105±0.13 (Fig. 4b). In Ow402, the best fit correlation was determined, associated with WR, Bt-1-1, Bt-2 and Bt-1-3 and yielded at 1129±13 Ma, MSWD = 0.68, with an initial ⁸⁷Sr/⁸⁶Sr ratio of 0.70227 ± 0.00028 for the Avebe tonalite (Fig. 4c).





4. DISCUSSION

Petrographic studies of tonalite and charnockite provided evidence of the coexistence of magmatic and metamorphic minerals in the So'o Group and NC. The first ones were residual clasts, representing a preserved magmatic flow in minerals while the second were blasts related to Eburnean thermotectonic events known in NyC border (Feybesse *et al.*, 1998; Penayé, 2004; Owona, 2008), Kibarian/Greenvalian or Panafrican close to the CAFB (Nzenti *et al.*, 1988; Mvondo Ondoa *et al.*, 2009; Owona, 2008; Owona *et al.*, 2011b). Clasts such as feldspars, pyroxene, opaque, apatite and zircon that form the S_1 foliation represent the Archean event E_1 . The MT-MP blasts as amphiboles occurred during the peak of the amphibolitic Eburnean event dominated by the ouralitization of pyroxene to amphibole. The LT-LP blasts as biotite, SGR feldspar and SGR-SGAR quartz (Kurse *et al.*, 2001; Stipp *et al.*, 2002; Passchier and Trouw, 2005; Owona, 2008) can be related to the Eburnean cooling phase or the Kibarian/Panafrican events. The saussuritization, damouritization, sericitization and chloritisation of minerals can be related to NC uplift and erosion.

The So'o Group like the whole NC, is dominated by the sub-vertical S_1 foliation suggesting that their emplacement was related to a sub-horizontal compression D_1 (Fig. 3a). The large-scale F_2 folds inferred the S_1 foliation folding and stereographic analyses support a sub-E-W compression with a sub-N-S transport of the "Archean nappe" as stated by the L_1 stretching lineation and A_2 fold axis oriented 355 30 (Fig. 2c; Owona, 2008; Owona *et al.*, 2011b). This Group was subjected to a brittle D_3 deformation represented by normal dip-slip faults oriented NNE-SSW, NNW-SSE, WNW-ESE and ENE-WSW under an overall crustal thinning as shown the by vertical σ_1 and horizontal sub-E-W σ_3 paleostress tensors (Fig. 2d; Owona, 2008; Owona *et al.*, 2011b).

The $^{207}\text{Pb}/^{206}\text{Pb}$ zircon age obtained from six grains without core for the Adzap charnockite in the So'o Group yielded reproducible Archean $^{207}\text{Pb}/^{206}\text{Pb}$ ages between 2762±6.9 Ma and 2722±15.1 Ma also as the $^{207}\text{Pb}/^{206}\text{Pb}$ ages between 2717±9 Ma and 2724±3 Ma (Shang *et al.*, 2010) with an isoplot weighted and corrected mean age of 2739±18 Ma (Fig. 4a). This age

is closer and slight older than 2722±2 Ma, interpreted as the minimum estimate of the crystallization age of the Sangmelima high-K granites (Shang *et al.*, 2010). Despite the very limited number, the single age obtained can be interpreted as the minimum estimate of the crystallization age of the Adzap charnockites in the So'o Group; younger than 3016±10 Ma to 2960±10 Ma for Sangmelima charnockites and 2896±7 Ma for Ebolowa charnockite in the NC and interpreted as charnockite protholith emplacement ages (Toteu *et al.*, 1994b; Tchameni, 1997; Tchameni *et al.*, 2000; Tchameni *et al.*, 2001; Shang *et al.*, 2001, 2004b, 2010; Owona, 2008). That youngest Archean age of Adzap charnockite in the So'o Group confirms demonstrated Pb losses in the Sangmelima Group extendable in the whole NC (Shang *et al.*, 2004a; 2010), which suffered minor reactivation during the Eburnean as well as the Panafrican tectonothermal events is represented by the ouralitization of pyroxene and various dynamic mineral recrystallization stages (Owona, 2008; Owona *et al.*, 2011a).

The $^{87}\text{Rb}/^{86}\text{Sr}$ -WR-Bt age from Adzap charnockite dated at 1969±170 Ma within error limits (Fig. 4b) confirms Paleoproterozoic ages previously obtained from the Sangmelima charnockite ($^{87}\text{Rb}/^{86}\text{Sr}$ -WR-Bt, 2299±22 Ma to 1997±19 Ma, Shang *et al.*, 2004a), and the Ebolowa syenite ($^{87}\text{Rb}/^{86}\text{Sr}$ -WR-Bt, 2349±1 Ma to 2321±1 Ma, Tchameni *et al.*, 2001) in NC as well as the Makoukou and Kinguele pegmatites from the Mont de cristal complex in Gabon ($^{87}\text{Rb}/^{86}\text{Sr}$ -WR-Bt, 2284±39 Ma to 1930±39 Ma, Caen Vachette *et al.*, 1988). It represents the cooling period of the Eburnean (2400-1800 Ma) tectonothermal event that slightly affected the NC (Feybesse *et al.*, 1998; Shang *et al.*, 2004a; Owona, 2008). The $^{87}\text{Rb}/^{86}\text{Sr}$ -WR-Bt age in the Avebe tonalite recorded for the first time in the NC that yielded at 1129±13 Ma can be assigned to the Kibarian/Greenvalian tectonothermal event (Fig. 4c). Considering the good MSWD value of that new age, it can be interpreted as the Kibarian/Greenvalian orogeny cooling period in the NC. The Kibarian/Greenvalian intermediate between the Eburnean and Panafrican tectonothermal events has certainly contributed to the NC reactivations and above Pb losses too. This orogeny already mentioned in the SW Cameroon (Feybesse *et al.*, 1987), needs to be confirmed by further occurrences

as in Sierra Leone (West Africa) dated at ca. 1349 Ma ($^{87}\text{Rb}/^{86}\text{Sr}$, Rollinson and Cliff, 1982 in Caen-Vachette *et al.*, 1988; Bertrand *et al.*, 1987).

5. CONCLUSION

The petrography of the charnockites and tonalites from the So'o Group in the NC has revealed their clast and blast minerals constitution. The $^{207}\text{Pb}/^{206}\text{Pb}$ evaporation zircon age obtained in Adzap charnockites from the So'o Group yielded 2739 ± 18 Ma confirms its Archean age and Pb loses during the NC Eburnean, Kibarian/Greenvalian and Panafrican reactivation, in agreement with previously published results. The Eburnean orogeny is represented by the orualitization of pyroxene, the feldspar and quartz blasts dynamic recrystallizations. This orogeny yielded with $^{87}\text{Rb}/^{86}\text{Sr}$ -WR-Bt method at 1969 ± 170 Ma in Adzap charnockites, interpreted as the Eburnean cooling age. The $^{87}\text{Rb}/^{86}\text{Sr}$ -WR-Bt has yielded at 11294 ± 13 Ma in Avebe tonalites, new in the So'o Group and NC, interpreted as the Kibarian/Greenvalian cooling time. The So'o Group involved in D_1 N-S compression emplacing the sub-vertical S_1 foliation and L_1 lineation. It experienced a D_2 E-W compression during the second E_2 tectonothermal event inducing SGR, SGAR feldspar and quartz, N-S large-scale F_2 folds and an "Archean nappe". The So'o Group and NC were affected at least by the brittle tectonic stage under an overall vertical shortening and sub-E-W horizontal extension. The final exhumation and erosion stage induced the damouritization, sericitization of feldspar and the chloritization of biotite in the NC.

ACKNOWLEDGMENT

The authors are grateful to the DAAD (German Academic exchange office) for financially supporting S. Owona's stay in Freiberg (Germany), to the members of the isotope laboratory, Institute of Mineralogy and those of the Laboratory of Tectonophysics, Institute of Geology of the TU-Bergakademie Freiberg for $^{207}\text{Pb}/^{206}\text{Pb}$ evaporation zircons and $^{87}\text{Rb}/^{86}\text{Sr}$ -WR-Bt dating and structural analyses. The constructive reviews by anonymous colleagues are also gratefully acknowledged.

6. Table captions

Table 1: Pb isotopic data from single grain zircon evaporation for Pb/Pb ages

Table 2: Rb and Sr isotopic data for Rb/Sr isochron ages

7. Figure captions

Fig. 1: (a) Geological sketch of the west-central Africa and South America connexion with cratonic masses and the Pan-African province of the Pan-Gondwana belt in a Pangea reconstruction modified from Castaing *et al.* (1994) and Ngako *et al.* (2003). CMR: Cameroon; CAR: Central African Republic; EG: Equatorial Guinea; CAFB: Central African Fold Belt; CCSZ: Central Cameroon Shear Zone; SF: Sanaga Fault. Blooded outline roughly marks the political boundary of Cameroon. (b) Southern Cameroon geological map (Modified after Champetier de Ribes *et al.*, 1956; Ngotué *et al.*, 2000; Ngako *et al.*, 2003; Penayé *et al.*, 2004; Nzenti *et al.*,

2006; Toteu *et al.*, 2006b; Thakounté *et al.*, 2007): NC: Ntem complex; NyC: Nyong Complex; SG: Sanaga Group; YG: Yaounde Group; DG: Dja Group; YoG: Yokadouma Group; SOG: Sembe-Ouessou Group. The location of study area (Fig. 2) is shown.

Fig. 2: The So'o Group sketch of lithology and faults showing the crustal shortening.

Fig. 3: The So'o Group (Ntem Complex) thematic sketches. (a) The sketch of foliation and its regional folding. (b) The sketch of lineation displaying its main SSE-NNW strike. NyC: Nyong Complex; OC: Oubanguide Complex. Poles of foliations S_n and axial planes A_{n+1} are plotted in equal area lower hemisphere that displays great circle of large scale folds F_n (Owona, 2008).

Fig. 4: The So'o Group new ages (Owona, 2008): (a) The $^{207}\text{Pb}/^{206}\text{Pb}$ zircons age and (b, c) $^{87}\text{Rb}/^{86}\text{Sr}$ isochron ages. a, b) sample Ow417 (Adzap charnockite) and c) sample Ow402 (Avebe tonalite).

8. Photo caption

Photo 1: The charnockites and tonalites granoblastic texture in XZ sections. Note the SGR quartz in Adzap charnockite (Ow417) with undulose extinction and SGR type-1 to -2 SGR feldspars. b) The complete recrystallization of old quartz1 in SGAR quartz2 grains in Avebe tonalite Ow402 (Owona, 2008).

REFERENCES

- Bertrand-Sarfati, J., Moussine-Pouchkine, A and Caby, R., 1987. Les corrélations du Protérozoïque au Cambrien en Afrique de l'Ouest: nouvelle interprétation géodynamique. *Bul. Soc. Géol., France*, 3, 855–865.
- Caen-Vachette, M., Vialette, Y., Bassot, J-P and Vidal, P., 1988. Apport de la géochronologie à la connaissance de la géologie gabonaise. *Chron. Rech. Min.* n° 491, 35-54.
- Castaing, C., Feybesse, J. L., Thieblemont, D., Triboulet, C and Chevremont, P., 1994. Paleogeographical reconstructions of the Pan-African/Brasiliano orogen: closure of an oceanic domain or intracontinental convergence between major blocks. *Precamb. Res.*, 69, 327-344.
- Champetier de Ribes, G and Aubague, M., 1956. Carte géologique de reconnaissance à l'échelle de 1/500.000, Feuille Yaounde-Est, avec notice explicative. *Dir. Min. Géol. Cameroun*, 35 p.
- Feybesse, J. L., Johan, V., Maurizot, P and Abessolo A., 1987. Evolution tectonométamorphique libérienne et éburnéenne de la de la partie NW du craton zaïrois (SW Cameroun). In: J. Matheis, G. Schandelmeier (Eds), *Current Research in African Earth Sciences*. Balkema, Rotterdam, pp. 9–12.
- Feybesse, J. L., Johan, V., Triboulet, C., Guerrot, C., Mayaga-Minkolo, F., Bouchot, V and Eko N'dong, J.,

1998. The West Central African belt: a model of 2.5-2.0 Ma accretion and two-phase orogenic evolution. *Precamb. Res.*, 87, 161-216.
- Kober, B., 1987. Single zircon evaporation combined with Pb+ emitter bedding for ²⁰⁷Pb/²⁰⁶Pb-age investigations thermal ion mass spectrometry, and implications to zirconology. *Contrib. Mineral Petrol.*, 96, 63-71.
- Kurse, R., Stünitz, H and Kunze, K., 2001. Dynamic recrystallization processes in plagioclase porphyroclasts. *J. of struct. Geology*, 23, 1781-1802.
- Lasserre, M and Soba, B., 1976a. Age libérien de granodiorites et des gneiss à pyroxène du Cameroun méridional. *Bull., B.R.G.M., 2è série, IV, I*, 17-32.
- Ludwig, K. R., 2001. Users Manual for Isoplot/Ex (rev. 2.49): A Geochronological Toolkit for Microsoft Excel. Berkeley Geochronology Center, Special Publication No. 1a, 55 p.
- Maurizot, P., Abessolo, A., Feybesse, A., Johan, J. L and Lecompte, P., 1986. Etude et prospection minière au Sud Ouest Cameroun. Synthèse des travaux de 1978-1985. - Rap. BRGM 85 CNRS 066, Orléans, 274p.
- Mvondo Ondoa, J., Mvondo, H and Bas den Brok, 2009. Pan-African tectonics in northwestern Cameroon: Implication for the history of western Gondwana. *Gondwana Res.*, 16, 163–164
- Nédélec, A., Nsifa, E. N and Martin, H., 1990. Major and trace element geochemistry of the Archean Ntem plutonic complex (South Cameroon): Petrogenesis and crustal evolution. *Precamb. Res.*, 47, 35 – 50.
- Ngako, V., Affaton, P., Nnangue, J. M and Njanko, T., 2003. Pan-African tectonic evolution in central and southern Cameroon: transpression and transtension during sinistral shear movements. *J. Afr. Earth Sci.*, 36, 207-214.
- Ngotué, T., Nzenti, J. P., Barbey, P and Tchoua, F. M., 2000. The Ntui-Betamba high-grade gneisses: a northward extension of the Pan-African Yaounde gneisses in Cameroon. *J. Afr. Earth Sci.*, 31, 369–381.
- Njonfang, E., Ngako, V., Kwekam, M and Affaton, P., 2006. Les orthogneiss calco-alcalins de Fouban–Bankim : témoins d'une zone interne de marge active panafricaine en cisaillement. *C. R. Geosci.*, 338, 606–616
- Nsifa, E. N and Riou, R., 1990. Post Archean migmatization in the charnockitic series of the Ntem complex, Congo craton, Southern Cameroon. 15th colloquium on African Geology, Publications Occasionnelle, CIFEG, 22, 33–36.
- Nsifa, E. N., Tchameni, R and Belinga, S. M. E., 1993. De l'existence de formation catarchéennes dans le complexe cratonique du Ntem (Sud-Cameroun). *Projet N°273, Archean Cratonic Rocks of Africa, Abstract volume*, 23p.
- Numbem Tchakounte, J., Toteu, S. F., Van Schmus, W. R., Pényaye, J., Deloule, E., Mvondo Ondoa, J., Bouyo Houketchang, M., Ganwa, A. A., White, M. W., 2007. Evidence of ca 1.6-Ga detrital zircon in the Bafia Group (Cameroon): Implication for the chronostratigraphy of the Pan-African Belt north of the Congo craton. *C. R. Geosci.*, 339, 2, 132-142
- Nzenti, J. P., Barbey, P., Macaudiere, J and Soba, D., 1988. Origin and evolution of the late Precambrian high-grade Yaounde gneisses (Cameroon). *Precamb. Res.* 38: 91–109.
- Nzenti, J. P., Kapajika, B., Wörner, G and Lubala, T. R., 2006. Synkinematic emplacement of granitoids in a Pan-African shear zone in Central Cameroon. *J. Afr. Earth Sci.* 45: 74-86.
- Owona, S., 2008. Archean, Eburnean and Pan-African features and relationships in their junction zone in the South of Yaounde (Cameroon). Ph.D. Th., Univ. Douala, 232p.
- Owona, S., Mvondo Ondoa, J., Ratschbacher, L., Mbola Ndzana, S. P., Tchoua, M. F and Ekodeck, G. E., 2011b. The geometry of the Archean, Paleo- and Neoproterozoic tectonics in the Southwest Cameroon. *C.R. Geosci.*, 343, 312–322.
- Owona, S., Schulz B., Ratschbacher, L., Mvondo Ondoa, J., Ekodeck, G. E., Tchoua, M. F and Affaton, P., 2011a. Pan-African metamorphic evolution in the southern Yaounde Group (Oubanguide Complex, Cameroon) as revealed by EMP-monazite dating and thermobarometry of garnet metapelites. *J. Afr. Earth Sci.*, 56, 125-139.
- Passchier, C. W and Trouw, R. A. J., 2005. *Microtectonics.* – Springer, 366 p
- Penayé, J., Toteu, S. F., Tchameni, R., Van Schmus, W. R., Tchakounté, J., Ganwa, A., Minyem, D and Nsifa, E. N., 2004. The 2.1 Ma West Central African Belt in Cameroon: extension and evolution. *J. of Afr. Earth Sci.*, 39, 159-164.
- Ratschbacher, L., Hackerb, B. R., Calvertc, A., Webbd, E. L., Grimmera, C. J., McWilliamse, O. M., Irelandf, T., Dongg, S and Hug, J., 2003. Tectonics of the Qinling (Central China): tectonostratigraphy, geochronology, and deformation history.

- Tectonophysics, 366 (2003) 1–53.
- Rollinson, H. R and Cliff, R. A, 1982. New Rb/Sr age determination of the Archean basement of Eastern Sierra Leone. *Precamb. Res.*, 17, N°1, 63p.
- Schulz, B., Bombach, Pawligns, K and Brätz, H., 2004. Neoproterozoic to Early-Palaeozoic magmatic evolution in the Gondwana-derived Autoalpine basement to the south of the Tauern Window (Eastern Alps). *International Journal of Earth Science. (Geol Rundsch)*, 93, 824-843.
- Shang, C. K., 2001. Geology, geochemistry and geochronology of the Archean rocks from the Sangmelima region, Ntem Complex, NW of Congo Craton, South Cameroon. Ph. D. Thesis, University of Tubingen, 313p.
- Shang, C. K., Liégeois, J. P., Satir, M., Frisch, W and Nsifa, E. N., 2010. Late Archaean high-K granite geochronology of the northern metacratonic margin of the Archaean Congo craton, Southern Cameroon: Evidence for Pb-loss due to non-metamorphic causes. *Gondwana Res.*, 18, 2-3, 337-355
- Shang, C. K., Satir, M., Nsifa, E. K., Liégeois, J. P., Siebel, W and Taubald, H., 2006. Archean high-K granitoids produced by remelting of earlier Tonalite–Trondhjemite–Granodiorite (TTG) in the Sangmelima region of the Ntem complex of the Congo craton, southern Cameroon. *Int J. Earth Sci (Geol Rundsch)*. DOI 10.1007/s00531-006-0141-3
- Shang, C. K., Satir, M., Siebel, W., Nsifa, E. K., Taubald, H., Liégeois, J. P and Tchoua, F. M. 2004a. Major and trace element geochemistry, Rb-Sr and Sm-Nd systematics of the TTG magmatism in the Congo Craton: Case of the Sangmelima region, Ntem Complex, Southern Cameroon. *J. of Afr. Earth Sci.* 40. 1-2, 61-79.
- Shang, C. K., Wolfgang, S., Muharrem, S., Funken, C and Mvondo Ondo, J., 2004b. Zircon Pb-Pb and U-Pb systematics of TTG rocks in the Congo Craton: Constraints on crust formation, magmatism, and Pan-African lead loss. *Bull. of Geosc.*, 79, N° 4, 205-219.
- Sperner, B and Ratschbacher, L., 1994. ATurbo Pascal program package for graphical presentation and stress analysis of calcite deformation. *Z. Dtsch. Geol. Ges.* 145, 414– 423.
- Sperner, B., Ratschbacher, L and Ott, R., 1993. Fault-striae analysis: a TURBO PASCAL program package for graphical presentation and reduced stress tensor calculation. *Comput. Geosci.* 19, 1361–1388.
- Stacey, J. S and Kramers, J. D., 1975. Approximation of terrestrial lead isotope evolution by a two-stage model. *Earth Planet. Sci. Let.*, 26, 207-221.
- Stipp, M., Stünitz, H., Heilbronner, R and Schmid, S. M., 2002. The eastern Tonale fault zone: a 'natural laboratory' for crystal plastic deformation of quartz over a temperature range from 250 to 700°C. *J. Str. Geol.*, 24, 3, 1861-1884.
- Tchameni, R., 1997. Géochimie et géochronologie des formations de l'Archéen et du Protérozoïque du Sud Cameroun (Groupe du Ntem, Craton du Congo). Th. Univ. Orléans, 356p.
- Tchameni, R., Megzer, K., Nsifa, N. E and Pouclet, A., 2000. Neoarchaean evolution in the Congo Craton: Evidence from K-rich granitoids of the Ntem Complex, Southern Cameroon. *J. of Afr. Earth Sci.* 30, 133-147.
- Tchameni, R., Mezger, K., Nsifa, N. E and Pouclet, A., 2001. Crustal origin of Early Proterozoic syenites in the Congo craton (Ntem complex), South Cameroon. *Lithos* 57, 23–42.
- Tichomirowa, M., Berger, H-J., Koch, E. A., Belyatski, B., Götze, J., Kempe, U., Nasdala, L and Schaltegger, U., 2001. Zircon ages of high-grade gneisses in the Eastern of Erzgebirge (Central European Variscides) – Constraints on origin of the rocks and Precambrian to Ordovician magmatic event in the Variscan fold belt. *Lithos* 56, 303-332.
- Toteu, S. F., Van Schmus, W. R., Pénaye, J and Nyobé, J. B., 1994b. U/Pb and SM/Nd evidence for Eburnean and Pan-African high-grade metamorphism in cratonic rocks of southern of Cameroon. – *Precamb. Res.*, 67, 321-347.
- Trompette, R., 1994. Geology of western Gondwana (2000-500 Ma). Pan-African-Braziliano aggregation of South America and Africa. – A.A. Balkema, Rotterdam, the Netherlands.
- Wiedenbeck, M., Alle, P., Corfu, F., Griffin, W. L., Meier, M., Oberli, F., Von Quadt, A., Roddick, J. C and Spiegel, W., 1995. Three natural zircon standards for U – Th – Pb, Lu – Hf, trace element and REE analysis. - *Geostand. Newsl.* 19: 1 – 23; London.